

**IDEA Article:**

**Simple electrode configurations for probing deep organs using Electrical Bio-Impedance techniques**

**K Siddique-e Rabbani**

Department of Biomedical Physics & Technology, University of Dhaka  
Dhaka 1000, Bangladesh  
Email: [rabbani@du.ac.bd](mailto:rabbani@du.ac.bd)

**ABSTRACT**

Tetrapolar Impedance Method (TPIM) and Focused Impedance Method (FIM) are two simple modalities of electrical bio-impedance measurement that could be employed to give useful physiological and diagnostic information of the human body. FIM is based on TPIM but uses a combination of two sets of TPIM, producing a focusing effect, which is useful to localize specific target organs. Most non-invasive electrical bio-impedance measurements based on TPIM and FIM use electrodes on one side of the body, outside the skin surface, which gives a shallow depth sensitivity. The sensitivity decreases with depth so that deep organs like lungs, heart, liver, stomach and bladder are not fully assessed through such measurements. Based on a long experience of studying electrical impedance methods, several qualitative ideas are presented in this article for probing deep organs using a few modified TPIM and FIM configurations. The suggestions are based on visualisations of both equipotentials and a popular sensitivity equation for transfer impedance, but not based on any quantitative analysis. Simulation and phantom studies based on these ideas may produce some practically useful electrode configurations for real life bio-impedance measurements.

Keywords: Electrical bio-impedance, deep organ bio-impedance, TPIM, FIM

**INTRODUCTION**

Body tissues have electrical properties which can be put to good use for physiological investigations of body functions, detection and diagnosis of health and disorder through measurements of electrical impedance. Historically, interest in bio-impedance flourished

particularly after the introduction of Tetrapolar Impedance Measurement (TPIM) technique, derived from Kelvin sensing using a four point probe for impedance measurements [Nyboer, 1959], which eliminates skin-electrode contact impedance that had posed a challenge before, since the contact impedance is usually very large compared to that of the bulk at typical measurement frequencies. TPIM essentially uses two electrodes for driving an alternating current and two other electrodes for measuring the potential developed between these points. The value obtained through dividing the measured potential by the driven current is known as ‘Transfer Impedance’ [Martinsen and Grimnes, 2009], which depends very much on the placement of the electrodes, the shape of the body (as a volume conductor) and the conductivity distribution inside. Therefore, different electrode placements will lead to different transfer impedance values. Since current flow through the human body is complex depending on the distribution of different organs and cell types, the measurements were mainly limited to a few whole body parameters like fat free mass, total body water, etc., through electrodes connected at extremities of the limbs [Lukaski, 1985, Kushner and Schoeller, 1986]. A significant leap in the interest in bioimpedance arose after the introduction of Electrical Impedance Tomography (EIT) [Henderson and Webster 1978, Barber, Brown and Freeston, 1983] which produced a 2D tomographic image using multiple TPIM measurements using 16, 32 or more electrodes fixed around a volume conductor. Of course initially it was called ‘Impedance Camera’ by Henderson and Webster and ‘Applied Potential Tomography (APT)’ by Barber, Brown and Freeston, the name EIT being chosen by the global community later. APT was initially explained through visualizations of sensitive regions based on equipotential lines passing through the two potential measuring electrodes. Later, a point sensitivity visualization was introduced by others based on sensitivity equations involving current density vectors originating due to both the two pairs of electrodes in TPIM [Grimnes and Martinsen 2015]. Developing a mathematical analysis based on a pair of current drive electrodes and a separate pair of potential measuring electrodes proved a challenge. Therefore, reciprocity theorem was invoked which says that swapping the current and potential electrode pairs would give the same value [Geselowitz 1971, Grimnes and Martinsen, 2015]. Since in each configuration, the sensitivity of a point to the total measurement is expected to be dependent on the current density at that point, the combined effect was defined through the scalar product of the two current density vectors,  $J_1$  and  $J_2$  at the point in question as,

$$S = \frac{J_1 \cdot J_2}{I^2} \quad \dots (1)$$

where the equation has been normalized through a division by the square of the magnitude of current  $I$ , assumed the same through both the electrode pairs. The contribution of any point to the total measured transfer impedance is then given as,  $\rho S$ , where  $\rho$  is the resistivity at the point in question. Therefore, the total transfer impedance  $Z_T$  is given by a volume integral over the whole of the volume concerned and is given by,

$$Z_T = \int \rho S \, dV \quad \dots (2)$$

However, 2D EIT image has contribution of objects from the 3<sup>rd</sup> dimension [Rabbani and Kabir, 1991] in a complex way, so individual pixel values do not represent the target distribution accurately. 3D EIT is currently under development, but it is much more complex and will take time before it comes into the clinical arena. The inroad of 2D EIT into the clinical arena is also slow because of the above limitations. Its major use has been in studying time dynamics of large organs integrating the pixel values within a region of interest representing the target organ.

Recently, Focused Impedance Method (FIM) was introduced as a bridge between TPIM and EIT [Rabbani et al 1999, Rabbani and Karal 2008, Isla, Rabbani and Wilson, 2010]. It can localize a target region using 8, 6 or 4 electrodes with complexity marginally greater than that of TPIM, and much simpler than that of EIT. FIM has shown success in localized lung ventilation and gastric emptying, giving similar results as obtained using 2D EIT. Depending on individual applications, the location and depth of target organ, etc., an appropriate version of FIM may be chosen. For a visualization of the focused region using FIM, both equipotential surfaces and sensitivity equations have been used, and it has been suggested that a combination of both gives a better visualisation [Rabbani, 2018].

For non-invasive applications, so far FIM has been applied from one side of the body as it is convenient from measurement point of view. So it was mainly targeted to organs at shallow depths from the skin surface. TPIM has also been similarly applied, particularly for large organs like lungs, from one side of the thorax, either from the front or from the back.

With more insight developed in getting a focused region, a renewed interest has grown in using TPIM and FIM to obtain localization of target organs through appropriate configurations of electrodes, which involve both positioning of electrodes and changing their sizes and shapes. This has led to new ideas for probing deeper regions of the body using TPIM and FIM and the present article presents some ideas which may form the basis of several such investigations. This paper does not give any outcome of simulation or experimental work. It just provides ideas for probing deep regions of the body for specific examples based on the understanding developed through a long experience on electrical impedance work. Other researchers may use these ideas for a more scientific study and the results may inspire investigators into using one or more of these modalities for their individual requirements, or innovate new ones.

## METHODS

As mentioned before, the ideas stem from a combination of visualisations based on both equipotentials (curved surfaces in 3D) and sensitivity equations. For the former, the equipotentials are plotted based on the current flux distribution for a particular electrode configuration and the volume conductor. The difference of potential between the two equipotential surfaces passing through the two potential electrodes gives the value of the relevant potential. This potential divided by the driven current gives the desired 'Transfer Impedance' which is specific to the volume conductor and the electrode configuration. The region within the two equipotentials contribute mostly to the measured transfer impedance.

Again, if one looks at equation 1, the sensitivity will depend on  $J_1 J_2 \cos \theta$ , where  $\theta$  is the angle between the two vectors. Therefore, S will depend on the magnitudes of the two currents and the angle between them. The following points are worth remembering for any visualization of electrical impedance.

- i. S will be high if both  $J_1$  and  $J_2$  have high values and have the same direction.
- ii. S will be zero at points where  $J_1$  and  $J_2$  are orthogonal to each other.

Based on all of the above means of visualization, the following ideas are put forward which may help in mental visualisation of new methods. The schematic figures shown in this work are based

mainly on intuition and previous experience of the author, and are mainly presented here as a suggestive starting point. One has to carry out rigorous analyses and experimental measurements to obtain the actual picture, with real values. Firstly, the basic visualization of a TPIM system is discussed here before going into the suggested new ideas.

Figure 1a shows a typical application of TPIM where the four electrodes are arranged in a linear array, current driven through the outer electrodes (red circles) while the potential is measured between the inner electrodes (blue circles). In a 3D volume conductor this may represent 2D cross-section through the electrode plane, which in typical applications, is on the surface of the volume conductor. The iso-current lines are shown schematically in solid red lines while the two equipotential lines passing through the potential measuring electrodes are shown dotted. However, the iso-current fluxes and the equipotentials would be curved surfaces in 3D, into the depth of the volume conductor, which are not shown here. The zone within the two equipotentials is usually taken to be the sensitive zone in the equipotential visualisation. An insulating object placed within

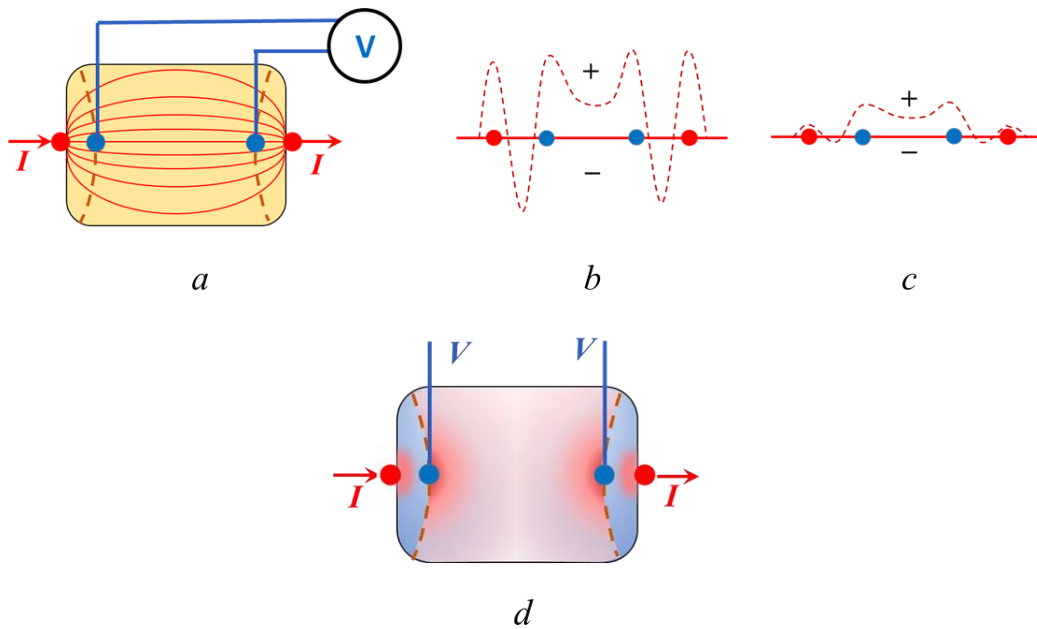


**Fig.1:** (a) Linear array TPIM showing iso-current lines and equipotentials passing through potential electrodes in the electrode plane. (b) Suggested schematic point sensitivity distribution along the line of the electrodes on the electrode plane, dotted line. (c) The upper side shows positive sensitivity (shown with a '+' sign while the lower part shows negative sensitivity shown with a '-' sign). Similar schematic sensitivity at a depth parallel to the electrode plane. (d) Combination of equipotential visualization and point sensitivity distribution in a plane parallel to the electrode plane. Negative sensitivity zones are shown in blue.

this region will increase the measured voltage, and hence an increased transfer impedance. This is called positive sensitivity. On the other hand, if an insulating object is placed in certain regions between the current and potential electrodes on both sides, the measured transfer impedance decreases, which is opposite to what is expected. This is called negative sensitivity. Along the line of the electrodes, the sensitivity however varies greatly, being high near the electrodes, which is suggested by the sensitivity equation. Fig.1b shows a suggestive schematic pattern of point sensitivity along this line. Positive sensitivity, shown upwards, is high around all the four electrodes, while the sensitivity is low in between the two potential electrodes, but positive. Negative sensitivity occurs between the current and voltage electrodes on both sides as the angle  $\theta$  happens to be greater than  $90^\circ$  in this region.

However as one goes down in depth, the relative sensitivity patterns change considerably, and get reduced in magnitude. Along a line parallel to the electrodes but at a depth, a suggestive schematic pattern of the point sensitivity is shown in Figure 1c. The high sensitivities around the electrodes reduce drastically. The negative sensitivity also decreases drastically. On the other hand, the positive sensitivity in between the two potential electrodes does not decrease so much and is more uniform throughout, which may be used to advantage.

The negative sensitivity of TPIM is a disadvantage. If a large object encompasses regions of both positive and negative sensitivity, the resulting change will be diminished depending on the percentage of the object falling within each of these regions with opposite sensitivity. However, in most applications one measures changes in the tissue parameters in time where such a change is expected, or with the change in frequency of the impedance measuring signal, where a change in the tissue parameter of the target object with frequency is expected. Therefore, if the electrodes are judiciously placed such that a single object is targeted which remains within the positive sensitivity zone, the effect of the negative sensitivity zone can be minimized. Since TPIM is still the basis of most electrical impedance based techniques as it can eliminate the contact impedances, one has to accept this disadvantage and configure the electrodes such that the negative effects are minimized.

Coming to the point sensitivity equations, these definitely represent the distribution more accurately. However, one may get carried away to a mistaken visualization which is explained

below. The regions near the electrodes have very high sensitivity since the current densities are very high there compared to regions away from the electrodes, which is usually shown using a colour contour image, a suggestive schematic is shown in Fig. 1d. This image tends to bring the focus near the high intensity areas and one may easily neglect the contribution of the low intensity regions away from the electrodes, near the middle of the conductor. However, one needs to appreciate that it is the total sum or integration of the sensitivity values which make the total impedance. Large volumes away from the electrodes may contribute significantly since the total integrated volume is large, even though the sensitivity values are very low in these regions.

On the other hand, the equipotential point of view tends to give an impression that the whole region between the equipotentials intersecting the potential electrodes contribute equally to the measured transfer impedance, which is obviously not true. Therefore, a practical solution would be to combine the two means of visualisation which will give a quick mental picture of the possibilities when one attempts at choosing a new configuration of electrodes for probing a deep organ of the human body.

### **Probing deep regions of the body**

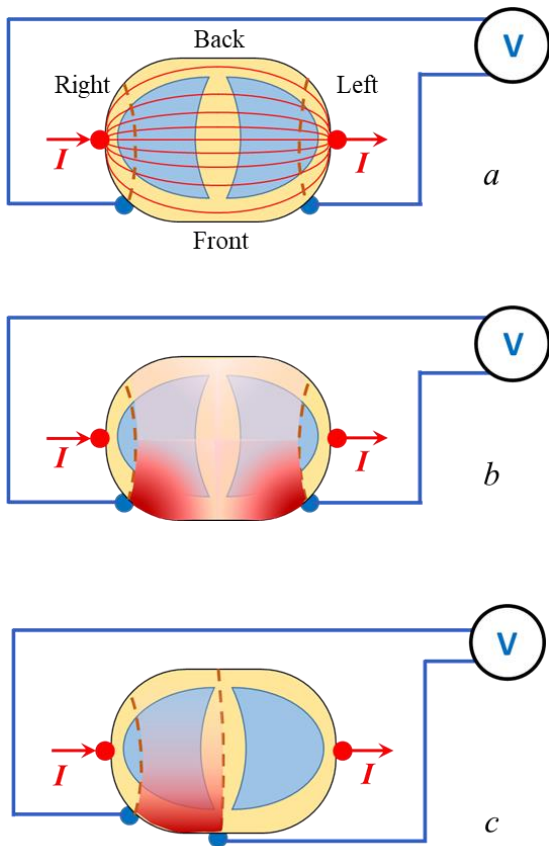
#### *Idea Examples and suggested sensitivity patterns*

Based on the above suggestions some ideas of electrode configurations targeting some typical deep organs are presented and explained through accompanied figures below.

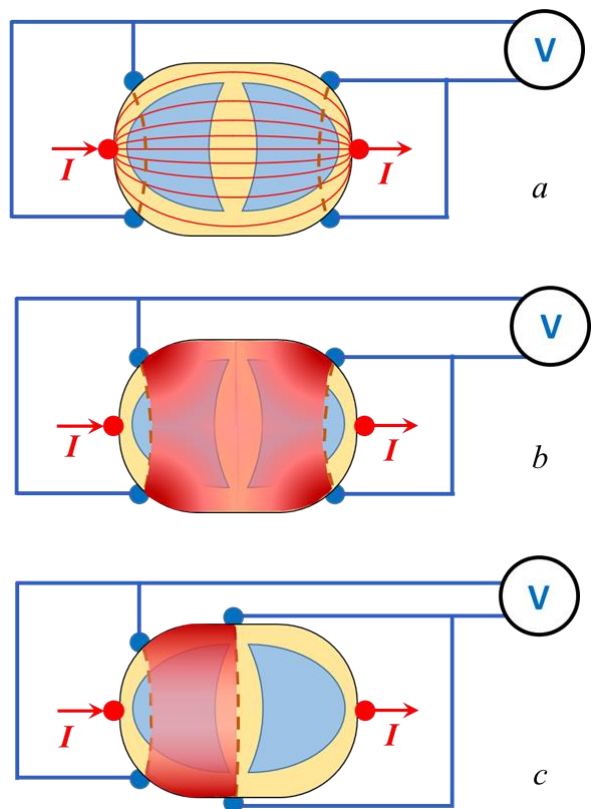
#### ***I. Typical configuration of TPIM in transverse plane***

Figure 2 shows a simplified representation of a transverse section of the upper thorax (viewed from the top) of a human body showing two lung regions (in blue). Here it is assumed that the TPIM electrodes are arranged in a linear array in the same transverse plane with current electrodes (red dots) at the two lateral extremes. The potential electrodes (blue dots) are arranged in two configurations, (i) to cover both lungs (Figures 2a, 2b) and (ii) to cover only the right lung (Figure 2c). Figure 2a shows both the iso-current lines and the equipotential lines while Figures 2b and 2c show only the equipotential lines. These would be typical models for the use of TPIM in lungs study. The equipotential visualisation suggests that the whole region between the two equipotential lines will contribute to the measurement while the sensitivity equation suggests a higher sensitivity

near the potential electrodes. Combining these two visualisations, an approximate sensitivity visualization scheme has been made up through the colour shading. However, these have not been made up from any analysis, these are suggestive ones based on intuitive visualization. It is also to be noted that the negative sensitivity zones have not been shown here. Figure 2*b* and 2*c* show that the measured values will have higher contributions from the front, gradually decreasing with depth; the middle and the backside of the lungs will have very little contribution.



**Fig 2:** Simplified schematic sensitivity representation of a transverse section of the upper thorax of a human body for shown electrode configurations. The two lungs are shown in blue. Suggested sensitivity magnitudes are shown colour shaded.



**Fig 3:** Simplified schematic sensitivity representation of a novel idea, a modified TPIM with two pairs of appropriately shorted potential electrodes at front and back, giving increased sensitivity throughout the lungs region (*b*) and throughout lungs of one side only (*c*).



## II. Modification of conventional TPIM for deep probing

Figure 3 shows a novel electrode configuration with a small modification to the typical conventional configuration discussed in the previous section, but which has the potential to increase the sensitivity of the deeper regions of the lungs significantly.

Here, two more potential electrodes are added and placed on the backside of the thorax exactly opposite to the ones in the front. The corresponding ones are shorted. Figures 3b and 3c show the suggested sensitivity patterns, Figure 3b for both the lungs and Figure 3c for right lung only. The potential electrodes on both the front and the back will have high sensitivity zones near them, as in Figure 2, which individually will gradually decrease to the opposite side. It is expected that this new arrangement will give addition of the two individual sensitivities in between, resulting in increased sensitivity in the mid-region. With respect to the depth of the thorax, at certain electrode separation the sensitivity may turn out to be almost uniform across the lungs region. The concept is similar to that of Helmholtz coils in electromagnetism. Thus this arrangement is expected to give adequate information throughout the depth of the lungs at any transverse plane. Of course, there will be contributions from a thick region extending to the 3<sup>rd</sup> dimension around the transverse plane. Using point electrodes, the iso-current lines in the 3<sup>rd</sup> dimension will also be curved, so the sensitive thickness will vary, being the greatest at the middle. Here, use of long strip electrodes can define the thickness of the sensitive zone better as shown in Figure 4. Along most of the length

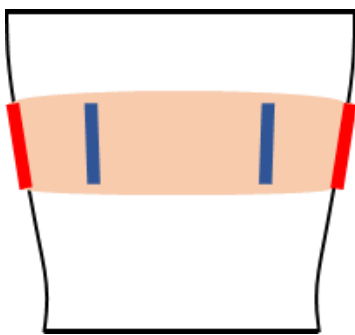


**Fig 4:** Having a thick sensitive zone with long strip electrodes

of the electrodes, the current lines will be almost parallel except at the upper and lower ends, like a fringing field pattern. Therefore, use of such long strip electrodes may be better to study different vertical thick segments of the lungs rather than targeting a thin slice.

## III. Biasing sensitivity to one side

If one is interested in measuring one side of the lungs (left or right) only, it may be advantageous to make the current density higher on the target side. A way of doing this would be to use a wide electrode on the opposite side as shown in Figure 5. As shown here, the current density will be higher near the smaller current electrode on the left, giving a better sensitivity for studies of the left lung using the

configuration of the potential electrodes. Often a wide electrode is impractical. In that case two electrodes on the right, shorted to make a single current electrode as shown in Figure 6 may give a similar outcome.

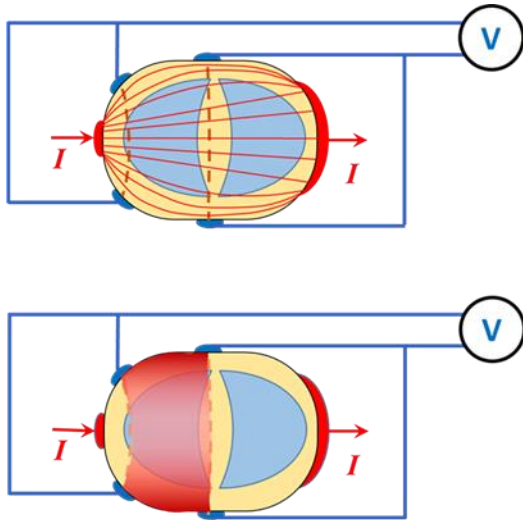


**Fig 5:** If the target segment is left lung, a wide current electrode on the right side will reduce the current density on the right, increasing the current density, hence, sensitivity on the left.

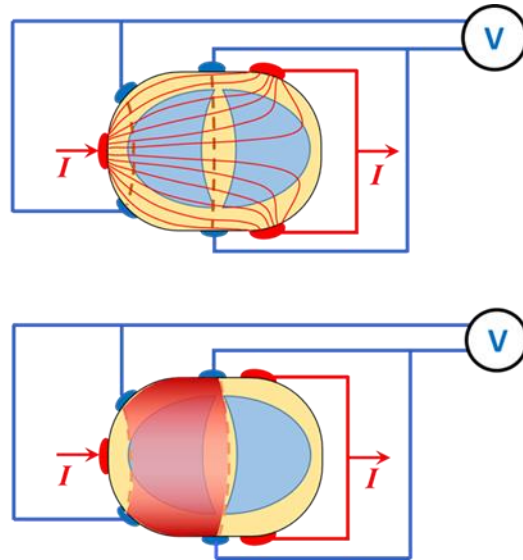


**Fig 6:** Use of two connected small electrodes instead of one wide electrode as used in Fig 5 to give reduced current density in the right, increasing sensitivity on the left side.

**IV. Use of FIM in a horizontal plane**

Use of Focused Impedance Method (FIM) [Rabbani et al, 1999, Rabbani and Karal, 2008, Rabbani, 2018] has been mainly applied to study objects at shallow depths, placing the electrodes on one side of the body. However, the technique of Four-electrode FIM (4-FIM) may be suitably arranged

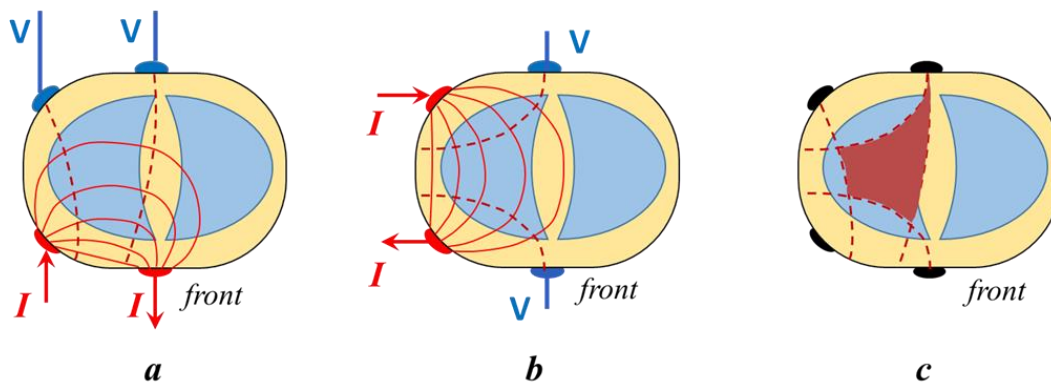


**Fig 7:** 4-FIM applied on a horizontal plane of the thorax, here, targeting the left lung. Equipotential viewpoint for the suggestion of the sensitive zone.

to give information in the deep regions of the body. Figure 7 shows a suggested arrangement for probing the deep regions of the left lung on a horizontal plane. Taking the lower side of the schematic cross section of the thorax as the front, the electrode arrangement shows 4-FIM to focus the left lung. Here the equipotential viewpoint is shown while that suggested on a combined viewpoint that includes the current density based sensitivity equation is shown in Figure 8.

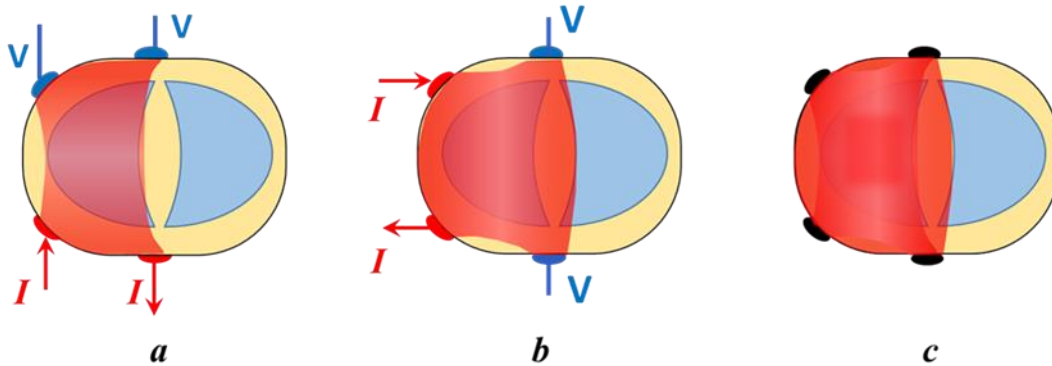


**Fig 8:** 4-FIM applied as in Fig 7, but sensitivity suggestion based on both equipotential and sensitivity equation

In the first step for this measurement, current is passed through the pair of electrodes in the front (red electrodes) while potential is measured across the pair in the back (blue electrodes). The iso-current lines (solid lines) due to the current electrodes and the equipotential lines (dashed lines) passing through the potential electrodes are shown in Figure 7a. In the next step of the measurement, current and potential electrodes are reorganized such that current is passed through the pair on the left and the potential is measured across the pair on the right (placed at the centre of the front and back in Figure 7b). Again, the new iso-current lines and the specific equipotential lines are shown. Assuming that the region between the two sets of equipotential lines shown in each case contains the sensitive volume, the region common to both will have enhanced sensitivity, as shown in Figure 7c. The equivalent suggested visualization considering the sensitivity equation is shown in Figure 8, for each of the separate electrode arrangements as above (Figure 8a and 8b) and the combined on in Figure 8c. This suggests a good sensitivity throughout the lung region, from front to back. Again, using long strip electrodes as shown in Figure 4, one may have an assessment of a thick lung region in the horizontal plane.

#### ***V. Targeting an asymmetrically placed object using modified TPIM***

If one wants to target an asymmetrically placed object such as the heart or stomach, a modified TPIM arrangement may be envisaged as shown in Figure 9. Here the target object is shown near the front, slightly to the left of the midline (blue ellipse). To increase sensitivity around this object, the current electrodes are organized as in Figure 6, but swapped laterally in order to increase the sensitivity on the side of the target object. In addition, the arrangement of the potential electrodes are made slightly different from that in Figure 6. The separation between the front pair of potential

electrodes is kept smaller than that at the back. This will increase the sensitivity towards the front as shown in Figure 9 (right figure). A similar concept may be used for objects close to any surface, either in the front, back, or on the sides.

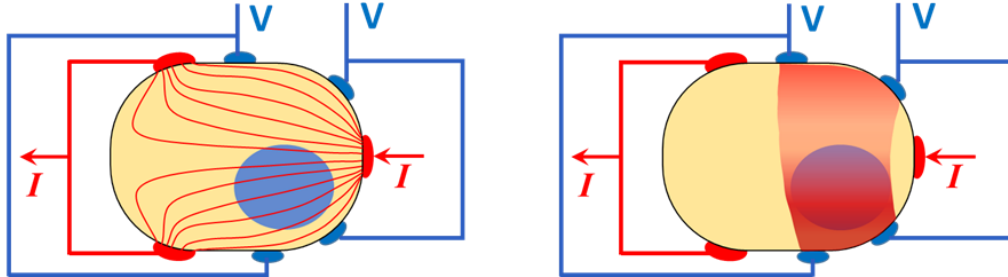


**Fig 9:** Modified TPIM as in Fig 6, but changing the separation of the potential electrodes on the front and the back, the sensitivity is enhanced towards the front. It helps target an object located towards the front.

### VI. Targeting an asymmetrically placed object using FIM

For asymmetrically objects as considered in the previous section, FIM may be used to advantage as well, increasing the sensitivity at the target organ further as shown in Figure 10. Here two TPIM configurations of electrodes are used separately and then the results are combined to get an 8-electrode FIM. Here,  $I_1$  represents the two current drive electrodes (red) for the first TPIM configuration for which  $V_1$  represents the two potential electrodes (blue). Again, the separation between the electrodes is less in the front, compared to that at the back. The equipotential lines passing through the two  $V_1$  electrodes are schematically shown as black dotted lines (Fig 10a). For the second TPIM configuration  $I_2$  represents the two current drive electrodes (red) and  $V_2$  represents the two potential electrodes (blue). Again, the separation between the electrodes is less in the front, compared to that at the back. The equipotential lines passing through the two  $V_2$  electrodes are schematically shown as green dotted lines (Figure 10a). Imagining the sensitive region based on equipotential lines, one would expect higher sensitivity within the zone bounded by the four dotted lines in Figure 10a, which encloses the target object, although some outside region is also enclosed.

To suggest visualisation based on the sensitivity equation, current is considered driven through both the current drive and potential measuring electrodes using an argument based on reciprocity theorem, as mentioned in the beginning. Here, the dashed lines between the pair of  $I_1$  electrodes and that between the pair of  $V_1$  electrodes indicate the lines of highest current between the respective pairs (Figure 10b). It may be visualised that between these two dashed lines, the current density vectors for the two currents have very small angles between them at most points, so the scalar product will have relatively high values compared to that at the points outside this region, giving higher sensitivity between these lines, as shown in Figure 10c. There will be fringing effects outside the dashed lines. Again, since the separation between  $I_1$  and  $V_1$  electrodes at the front is

less than that at the back, the sensitivity would be higher in the front. Similarly, for the other TPIM involving  $I_2$  and  $V_2$  electrodes the sensitivity will be similarly high in the front, gradually reducing towards the back. Now adding these two point sensitivity distributions one will come up with a situation shown in Figure 10c, where the sensitivity will be high in the region of the target object and around, but less at the back. Thus suitable choice of electrode placement will allow one to focus target organs deep inside the body.

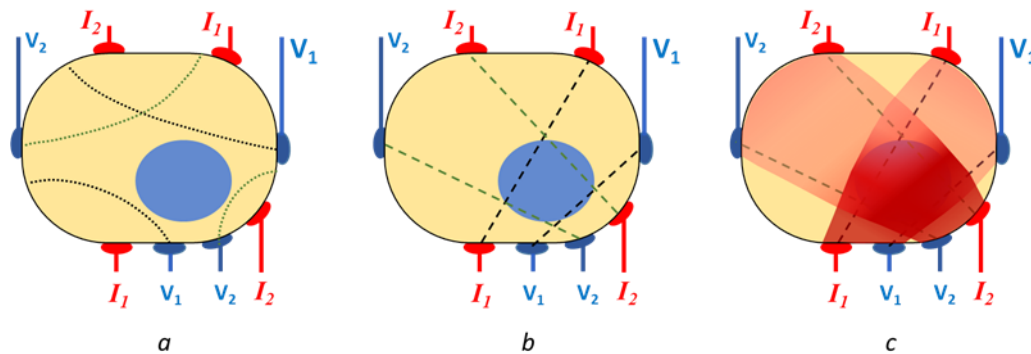


**Fig 10:** 8-electrode FIM to localise asymmetrically placed target object. Equipotential line visualisation (a). Current path visualisation, showing respective maximum current lines (b). Visualisation of sensitivity distribution based on sensitivity equation (c). Enhanced sensitivity for the combined distribution expected at the position of the target object.

## DISCUSSIONS

Although the ideas presented in this article are all hypothetical, they are based on sound logic and arguments, obtained through a long experience of working in the relevant field. The distributions shown in colour are not accurate representations of the expected results, but these are suggestive and one should try out these ideas through finite element method (FEM) simulation first and then through measurements on phantoms. For real life applications in the human body, further adjustments will be needed as the distribution of the internal organs are very complex and it is almost impossible to reproduce these in simulations or in phantoms. Besides, variations do occur from person to person and from health to disorder.

In the colour distribution diagrams, only positive sensitivities are suggested, negative sensitivities are not shown (except for Figure 1). One will obtain these clearly in a FEM simulation.

Thus, for probing any deep organ of the body one may need to innovate newer electrode placements and measurement modalities, but the ideas presented in this article will help a great deal in coming to a design with a minimum effort.

## ACKNOWLEDGEMENTS

The author acknowledges the wholehearted support of the group in Sheffield, UK, the pioneers of EIT measurements on the human body, which had helped the author in building up necessary background, knowledge and experience in Electrical Impedance measurements, eventually leading to the innovation of FIM at Dhaka. The author acknowledges the then British Overseas Development Agency to sponsor this link with Sheffield. The author is ever indebted to Professor M S Islam of the Department of Physics of the University of Dhaka to invite the author in joining him in building up the pioneering group on Biomedical Physics Research in Bangladesh, which eventually led to the academic link with Sheffield University. The author acknowledges the contributions of a host of students at the University of Dhaka who worked with him for at different times over a few decades that advanced the work on FIM to an international level. Finally the author would like to acknowledge the International Science Programme of Uppsala University, Sweden, for the continued financial support since 2011 to carry on the research work at the author's department at Dhaka University.

## REFERENCES

- Barber DC, Brown BH, Freeston IL, 1983. Imaging spatial distributions of resistivity using applied potential tomography. *Electron. Lett.* (19) 933–935.
- Cheney M and Isaacson D, 1995. Issues in electrical impedance imaging. *Computing in Science and Engineering*, 2(4), 53–62.
- Geselowitz DB, 1971. An application of electrocardiographic lead theory to impedance plethysmography. *IEEE Trans. Biomed. Eng.* 18: 38–41
- Grimnes S and Martinsen ØG, 2015. *Bioelectricity and Biomedance Basics*, Elsevier.
- Henderson RP and Webster JG, 1978. An Impedance Camera for Spatially Specific Measurements of the Thorax, *IEEE Transactions on Biomedical Engineering*, 25(3) 250 – 254.  
DOI: 10.1109/TBME.1978.326329
- Islam N, Rabbani KS and Wilson AJ, 2010. The sensitivity of focused electrical impedance measurements, *Physiol. Meas.* 31:S97–S109. doi:10.1088/0967-3334/31/8/S08.
- Kushner RF and Schoeller DA, 1986. Estimation of total body water by bioelectrical impedance analysis, *The American Journal of Clinical Nutrition*, 44 (3) 417–424, <https://doi.org/10.1093/ajcn/44.3.417>.
- Lukaski HC, Johnson PE, Bolonchuk WW and Lykken GI, 1985. Assessment of fat-free mass using bioelectrical impedance measurements of the human body. *Am J Clin Nutr.* 41(4) 810-817.
- Martinsen ØG and Grimnes S, 2009. The concept of transfer impedance in bioimpedance measurements. In: Vander Sloten J., Verdonck P., Nyssen M., Hauelsen J. (eds) *4th European Conference of the International Federation for Medical and Biological Engineering*. IFMBE Proceedings, vol 22. Springer, Berlin, Heidelberg.
- Nyboer J, 1959, *Electrical Impedance Plethysmography*, Publisher: Charles C. Thomas, Springfield, IL.

Rabbani KS and Kabir H, 1991. Studies on the effect of the third dimension on a two dimensional Electrical Impedance Tomography system, *Clin Phy & Physiol Meas*, 12,393-402.

Rabbani KS, Sarker M, Akond MHR and Akter T, 1999. Focused Impedance measurement (FIM) - A new technique with improved zone localization. In: *Electrical Bioimpedance methods, Annals of the New York Academy of Sciences*, Volume 873, p.408 to 420. published online: 6 FEB 2006 ,DOI: 10.1111/j.1749-6632.1999.tb09490.x.

Rabbani KS and Karal MAS, 2008. A new four-electrode Focused Impedance Measurement (FIM) system for physiological study. *Annals of Biomedical Engg (Springer, US)*. 36(6),1072-1077.

Rabbani KS, 2018. Focused Impedance Method: Basics and Applications. In: Simini F., Bertemes-Filho P. (eds) *Bioimpedance in Biomedical Applications and Research*. Springer, Cham, pp. 137-185. [https://doi.org/10.1007/978-3-319-74388-2\\_9](https://doi.org/10.1007/978-3-319-74388-2_9), ISBN (Print): 978-3-319-74387-5.